The IRS 1 Circumstellar Disk, and the Origin of the Jet and CO Outflow in B5

W. D. Langer[1], J. Velusamy, and T. Xie[2]

MS 169-506, Jet Propulsion Laboratory, California Institute of Technology, Pasadena, CA 91109

Received _____ ; accepted _____

[1]langer@langer.jpl.nasa.gov

[2]Present address: Department of Astronomy, University of Maryland, College Park, MD 20742

ABSTRACT

We report the discovery of the inner edge of the high velocity CO outflow associated with the bipolar jet originating from IRS 1 in Barnard 5 and the first ever resolution of its circumstellar disk in the 2.6111111 dust continuum and CO isotopes. From high spatial resolution observations made with the Owens Valley Millimeter Array we are able to locate the origin of the outflow to within 350 AU on either side of IRS 1 and apparently at the edge of, or possibly within, its circumstellar disk. The orientation of this disk in the continuum is exactly perpendicular to the highly collimated jet outflow recently seen in optical emission at much further distances. The ^{12}CO interferometer maps show two cone-like features originating at IRS1, the blue one fanning open to the northeast and the red one to the southwest. The vertices of the cones are on either side of the circumstellar disk and have an opening angle of $\sim 90°$. ^{13}CO is optically thick in the interferometer map and traces the gas far outside the IRS 1 circumstellar disk. The less abundant $C^{18}O$ almost certainly probes part of the disk structure and its extended circumstellar envelope, but it too is optically thick at the center of the disk. Our HCO^+ map traces an extended disk of material rotating clockwise around a SW NE axis. The corresponding HCN map is associated with the outflow material and ambient core, but not the disk. These dense gas tracers indicate significant chemical differentiation in the circumstellar region on small scales.

Subject headings: stars: pre-main sequence - individual (B5 IRS1); ISM: jets and outflows

1. INTRODUCTION

IRS] is the most luminous and most deeply embedded of the four infrared sources identified as low mass young stellar objects (YSOs) in Barnard 5. Goldsmith, Langer, & Wilson (1 986) detected high velocity C() outflows associated with IRS 1, IRS 2 and IRS 3 and suggested that IRS 4, located in a cavity, was in a post outflow stage. They proposed that these formed a sequence of YSOs at different stages of evolution with IRS 1 the youngest and IRS 4 the oldest. They also suggested that B5 was undergoing self-limited star formation and that the ongoing star formation was causing chemical evolution as a result of fragment-interclump recycling. The dense star forming interior, as traced by $C^{18}O$, has a mass of **'200** to 500 $M_{\odot}$ (Langer et al. 1989) and the core surrounding IRS 1 is estimated to have about 50 $M_{\odot}$, assuming a distance of 350 pc.

The structure of the core region surrounding IRS 1 was investigated in more detail by Fuller et al. (1 991) using higher spatial resolution observations. These authors made a beam sampled map of the high velocity outflow traced by ^{12}CO (1 - › *O)* using the IRAM 30m antenna, with a beamsize of 22". They detected CO outflow material out to a velocity of ± 10 km s^{-1} with respect to the rest velocity of the ambient gas, but could not trace its origin to better than 20" around IRS 1. The shape of the CO outflow appears in projection as a narrow arc with opening angle about 30°. In the blue lobe they noted that the location of the apex of the arc corresponded closely with that of an optical arc seen at the Gunn i-band by Heyer et al. (1990). The apex of the optical arc lies near IRS 1 and is apparently a reflection nebula illuminated by IRS1 (Moore & Emerson 1992). No comparable arc was detected at the Gunn i- band in the red-lobe of the out flow. Recently Bally, Devine, & Alten (1996) detected a high velocity optical jet associated with the CO outflow in B5 from observations of Hα and SII. This feature, which extends from ∼ 4' to 11' on both sides centered on IRS 1, could not be traced within several arcminutes of IRS 1 because of the

high optical extinction in the core, but points back to IRS 1.

In this *Letter* we present a new picture of the B5 innermost core using high spatial resolution observations of CO isotopes, dust continuum, and dense gas tracers HCO^+ and HCN made with the Owens Valley Radio Observatory Millimeter Array. We are able to trace tile high velocity CO outflow lobes back to their origins which lie within 1" of IRS 1 and within its circumstellar disk. Our HCO^+ observations trace the circumstellar disk and its surroundings and show that it is rotating about its axis. The HCN emission does not trace the disk and there appears to be significant chemical differentiation in this region.

2. OBSERVATIONS

The results presented here are based on observations made between April 1993 and May 1994 with the Owens Valley Millimeter Array (OVRO-MMA) which is operated by the California Institute of Technology. For the Spring of 1994 observing season the MMA was comprised of 5 antennas while the earlier observations had 4 antennas. We used SIS receivers with a single sideband (SSB) system temperature typically in the range of 250 to 400 K. Spectral line observations at $^{13}CO(1\rightarrow0)$ and $C^{18}O(1\rightarrow0)$ were obtained simultaneously using a 128 channel digital correlator. For each line 64 channels were used, giving a spectral resolution of 125 kHz (0.34 km s^{-1}). The $^{12}CO(1\rightarrow0)$ observations were taken with two different spectral resolutions, 125 and 500 kHz, each using 64 channels. The $HCN(1\rightarrow0)$ and $HCO^+(1\rightarrow0)$ observations were taken using spectral resolutions of 250 and 84 kHz, respectively. The continuum data were acquired simultaneously with the spectral line observations using 1 GHz bandwidth. The radio source 3C84 was used for gain and phase calibration. During each observing day four positions in B5 were observed with phase centers corresponding to the locations of the four infrared sources IRS 1 to 4. Observations of Uranus and 3C273 were used for flux calibrations and 3C273 was used for passband

calibration. The raw visibilty data were calibrated using software specific to OVRO-MMA (Scoville et al. 1993) and the maps were made using AIPS. Here we will only discuss our results for IRS1, as We did not detect significant emission from the other three sources.

3. RESULTS

3.1. Dust Emission Continuum and CO Isotope Maps

To resolve the disk emission we used the full resolution possible with the visibility data by using uniform weighting. Figure] shows the 2.6 mm continuum map made at 2".9 x 2".4 resolution. At the center is an elliptical disk oriented southeast-northwest with FWHM of 3".5 x 2".2 as determined from a 2-]) gaussian fit to the emisssion distribution. The center of the continuum emission is within 1" from the location of IRS1 (see '1'able 1) as determined by IRAS (Beichman et a]. 1984). Note there are several values in the literature for the position of IRS1, differing by as much as 2"-4", but within their respective measurement errors - see Table] If the circumstellar disk is centered on the YSO then the position of IRS 1, as determined from our continuum observations, should be RA(1950)= $03^h44^m32^s.00$ and DEC(1950)=$32°42'30''.0$, closest to the IRAS measurement of Beichman et al. (1 984).

'J'here is some indication of a. weak extended envelope surrounding the disk in the continuum map. The orientation of this disk in the continuum is exactly perpendicular to the large scale CO outflow (Fuller et al.) and the highly collimated jet outflow recently seen in optical emission (Bally et **al.**) at much further distances. Wc also detected weak continuum emission at 3.4 mm, ~ 3.5 mJy $(\text{beam})^{-1}$ at the IRS1 position, however it has a low signal to noise ratio of ~ 3. The 3.4 mm continuum data had only 500 MHz of continuum bandwidth (compared to]GHz at 2.6 mm) and a lower angular resolution of $\sim$

6“, and we do not have the sensitivity for comparison with the 2.6 mm map

The interferometer maps of $C^{18}O$ and ^{13}CO are shown in Figure 1 at 5“ x 4“ resolution. The $C^{18}O$ emission appears to trace the dense circumstellar disk seen in the continuum emission, as well as the surrounding gas. The structure and orientation of the inner region of the $C^{18}O$ map resembles that of the continuum map. To determine the physical properties we have fitted the central emission in each map with a 2-1) Gaussian. Table 1 summarizes the position, size, and position angle of the major axis of the disk emission in the continuum and CO isotope maps. The larger beam size in the CO maps and contamination from the surrounding core (and perhaps outflow) are probably responsible for some of the differences between them. Note that in the interferometer maps the larger scale emission from the B5 core (Langer et al. 1989) is resolved out and only the small scale emission from the disk and its surrounding are seen. The $C^{18}O$ emission is quite elongated (it covers 10“) and can be seen to extend much further than the continuum emission. This extended component may represent the surrounding core material from which IRS 1 arose. The ^{13}CO emission map shows less clearly the circumstellar disk component, and extends over a slightly larger region (see g’able 1) than that of the $C^{18}O$ extended emission. This isotope has a greater opacity than $C^{18}O$ and so it is not surprising that it does not probe the gas properties in the deeply buried disk or even in the dense core. Furthermore the ^{13}CO map could contain some of the emission from the outflow material.

3.2. ^{12}CO Emission

The ^{12}CO interferometer emission is presented in Figure 2 as spatial maps at three velocity intervals corresponding to the blue shifted, ambient, and red shifted gas. The major axis of the disk is almost exactly perpendicular to the jet outflow direction. It can be seen that the ^{12}CO ambient emission (Fig. 2b) peaks very close to that of the dust

continuum but is somewhat more extended along the direction perpendicular to the major axis of the disk. Therefore it appears to be tracing the out flow seen at velocities close to the rest velocity. Of course one does not expect to see the ^{12}CO emission from the disk and its surroundings as it is very opaque,

The ^{12}CO interferometer maps show two cone-like features originating at IRS 1, the blue Wing one fanning open to the northeast (Fig. 2a) and the red wing one open to the southwest (Fig. 2c), both with opening angles $\sim 90°$. It is also very striking to see in these maps that the vertices of the cones, the apex of the outflows, are located on either side of the dust continuum showing the origination of the flows at the top and bottom edges of the disk, within 1" (350 AU) of IRS 1, assuming a distance of 350 pc. Thus it would appear that we have traced the origin of the CO outflows back to the edge of the circumstellar disk and perhaps within the disk.

3.3. HCO^+ and HCN

The HCO^+ emission in the core of B5 is strong enough to resolve the central structure as a function of velocity. Figure 3 shows the interferometer maps of B5 in three velocity channels. The emission map is centered on the peak in the dust emission (to within the resolution limits of this map, which is larger than that of the continuum emission). HCO^+ appears to trace the circumstellar disk but also has a larger, more extended component (see Table 1). There is an apparent velocity shift in these maps indicative of clockwise rotation about an axis through the disk and parallel to the outflow axis corresponding to a gradient of 0.5 km S^{-1} over 2000 to 3000 AU.

The HCN emission, in contrast to the HCO+ emission, is not centered on IRS 1 and the circumstellar disk. In Figure 4 we present spatial maps of HCN made with different hyperfine components: 1) F=2→1, the main hyperfine line; and, 2) the sum of the weaker

components F=0→1 and 1- ›1. The HCO^+ map integrated over all velocities is shown for comparison. Fuller et al. determined from a two component gas layer model that the main component in HCN was optically thick. Thus by looking at the maps made in tile different hyperfine components we can see whether opacity effec ts might be affecting the position of the spatial distribution of the emission. The HCN emission in both maps is displaced to the cast of IRS 1, which sits near the edge of the distribution), and is distinctly different from the distribution seen in HCO^+. The similarity in both HCN maps argues then that this displacement is real and not an artifact of opacity. This shape of the HCN emission is similar to that observed by Fuller et al. but here the much higher resolution of our maps demonstrates unambiguously that HCN has little to do with IRS 1 or the circumstellar disk.

4. DISCUSSION

The observations presented here pr ovide striking evidence for the structural relationships of the IRS1 source, circumstellar disk, optical jet, and for the origin of the high velocity CO outflow (Figure 5 is a schematic of these components. The vertices of the red and blue shifted outflow lobes are separated by 4 ".5, They ar e oriented at a 73° position angle which is close to that of the optical jet (Bally et al.) and rotation axis (inferred from our HCO^+ data). In Figure 2b the emission from the ^{12}CO outflow gas at the rest velocity, peaks between the vertices of the red and blue lobes. Furthermore, its centroid is slightly shifted towards the red vertex. At the rest velocity the emission from both vertices will be close together and is seen as a single extended component due to smoothing by the beam. Therefore, the location of the rest velocity emission is consistent with the outflow originating at the vertices shown in Figures 2a&c and Figure 5. We conclude unambiguously that the bipolar outflow (and by inference the optical jet) originates with in 350 AU (l") from the star. The openings of the outflow cones continue out to at least 25"

(9000 AU), which is the edge of the field mapped by OVRO-MMA. At the edge of this field the width of the emission cone is 40" (14 ,000" AU). Beyond this the emission is traced in the large scale CO outflow maps (Goldsmith et al. and Fuller et al.),

To estimate the mass of the disk we use the $C^{18}O$ and continuum emission. Each has its own intrinsic uncertainties due to assumptions about abundance, temperature, and in the case of CO, opacity. The ratio of the brightness of ^{13}CO to $C^{18}O$ emission in the central disk region is $\sim$1.] , and the ^{13}CO emission is definitely optically thick. Even $C^{18}O$ probably has a $\tau \geq 1$ in the disk, which is consistent with the larger extent of the disk in $C^{1*}O$ compared to the continuum ('J'able 1). The peak brightness temperatures are 3.3 K for $C^{18}O$ and 2.9 K ^{1}for O. As the densities are high enough to thermalize the gas and $\tau \geq 1$ we have assumed a gas kinetic temperature 1 0 K. For an optical depth of 1 for $C^{18}O$, we estimate the mass of the disk to be 0.05 and 0.10 $M_\odot$ out to 3" and 6", respectively, using the equation in Chandler et al. (1 994).

From the 2.6 mm continuum flux we estimate the mass of the dust in the circumstellar disk (see Chandler et al. 1995) to be $\sim$ 0.10 and 0.17 $M_\odot$ out to 3" and 6" radius, respectively. We have assumed optically thin emission, a dust temperature of 30 K (Beichman et al.), and β= 1 The close agreement of the disk mass derived from the dust emission and the gas emission may be coincidental considering the uncertainties. However, taken at face value, it suggests that the continuum and $C^{18}O$ line emission trace roughly the same material and that $C^{18}O$ is not significantly depleted.

Comparing the distribution of HCN and HCO^+ (Figures 3 and 4) we see that they have very different distributions, whereas the HCO^+ is better correlated with ^{13}CO and $C^{18}O$. 'I'he correlation of HCO^+ is to 'be expected given that HCO^+ is produced from CO in the gas phase ion-molecule chemistry. Furthermore, the correlation in the distribution also indicates that the density is rather high in the region of $C^{18}O$ emission because HCO^+

requires high densities for collisional excitation. The lack of 11 CN emission around and within the disk is probably due to depletion of HCN onto grains, which is likely to be very efficient at such high densities if the grains are not too warm (Bergin et al. 1995). These results for HCN appear to be similar to what has been seen in CS in disks and their surrounding cores (Blake, van Dishoeck & Sargent 1992) and in CCS in the collapsing envelope around the YSO and disk in B335 (Velusamy, Kuiper & Langer 1995). HCN, CS, and CCS have large dipole moments, and are much more likely to stick on grains than CO.

In summary, our observations show that the red and blue shifted CO outflow originates on either side of the circumstellar disk centered on IRS 1 and within 350 AU of the central star. The opening angle at the disk edge is $\sim$ 90° and extends out to 10'' AU. At larger distances the Bell Labs and IRAM data show that the flow narrows to $\sim$ 30° between (3-6) x 10'' AU. The large opening near the source and narrowing of the CO outflow at large distances is consistent with models of a high velocity jet generating a turbulent mixing layer which expands outwards and can be traced by CO (see Biro & Raga 1994 and references therein). The size of the opening angle near the disk is consistent with the models of Cabrit & Bertout (1986) of a cone of expanding material emerging at an inclination angle to the line of sight between 30° and 60° (cf. Feibig et al. 1996).

The OVRO observations would not have been possible without the help and advice of the Caltech and OVRO staff, especially G. Blake, C. Chandler, A. Sargent, N. Scoville, and M. Yun. We would like to thank John Bally for providing preliminary results of the detection of an optical jet in B5. The Owens Valley Radio Observatory Millimeter Array is supported by NSF grant AST 93-1401/9, the K. T. and E. L. Norris Foundation, and the JPL Director's Research Discretionary Fund. This work was performed at the Jet Propulsion Laboratory, California Institute of Technology, under contract with the National Aeronautics and Space Administration.

REFERENCES

Bally, J., Devine, D., & Alten, V. 1996, submitted to ApJ Letters

Beichman, C. A., et al. 1984, ApJ, 278, L45

Biro, S. & Raga, A. C. 1994, ApJ, 434, 221

Blake, G. A., van Dishoeck, E. F. & Sargent, A. 1992, ApJ, 391, 199

Cabrit, S. & Bertout, C. 1986, ApJ, 307, 313

Chandler, C. J. & Sargent, A. I. 1993, ApJ, 414, L29

Chandler, C. J., Koerner, D. W., Sargent, A., I., & Wood, D. O. S. 1995, ApJ, 449, L139

Feibig, D., Duschl, W. J., Menten, K. M. & Tscharnuter, W. M. 1996, in press

Fuller, G. A., Myers, P. C., Welch, W. J., Goldsmith, P. F., Langer, W. D., Campbell, B G., Guilloteau, S., & Wilson, R W. 1991, ApJ, 376, 135

Goldsmith, P. F., Langer, W. D. & Wilson, R. W. 1986, ApJ, 303, 11

Heyer, M. H., Ladd, E. F., Myers, P. C., and Campbell, B., 1990, AJ, 99, 1585

Langer, w. D., Wilson, R. W., Goldsmith, P. P., & Beichman, C. A. 1989, ApJ, 337, 355

Moore, T. J. T. & Emerson, J. P. 1992, MNRAS, 259, 381

Scoville, N. Z., Carlstrom, J. E., Chandler, C. J., Phillips, J. A., Scott, S. L., Tilanus, R. P. J., & Wang, Z. 1993, PASP, 105, 1482

Velusamy, T., Kuiper, T. B. H., & Langer, W. D. 1995, ApJ, 451 L75

This manuscript was prepared with the AAS LaTeX macros v3. O.

Table 1: Gaussian Fit to IRS1 Disk and Core Emission

Transition	Position[a]		Size		
	RA(1950)	Dec(1950)	Major axis	Minor axis	Position Angle
	03^h44^m	$32°42'$	(")	(")	(^{0})
2.6 mm	$3 2^s.00 \pm 0.03$	$30".0 \pm 0.2$	*3.5 :10.4*	2.2 ± 0.4	146320
$C^{18}O(1\text{-}0)^b$	$3 1^s.92 \pm 0.02$	$31". "(\pm 0.2$	10.1 ± 0.4	3.0 ± 0.3	151 ± 4
$^{13}CO(1\text{-}0)^c$	$3 1^s.94 \pm 0.03$	$29".5 \pm 0.3$	12.2 ± 0.5	2.8 ± 0.3	5 ± 4
$HCO^+(1\text{-}0)^d$	$32^s.02 \pm 0.04$	$31".5 \pm 0.3$	17.9 ± 1.0	12.9 ± 0.6	5 ± 148
$2\ \mu m^e$	$31^s.80$	$32".0$			
$25\mu m^f$	$31^s.90$	$32".0$			

a. Listed errors are derived from the gaussian fit

b. Possibly confused by an extended envelope

c Possibly confused by an extended envelope and the outflow

d Possibly confused by an extended envelope and the core emission

e Fuller et al. 1991

f. Beichman et al. 1984

Fig. 1

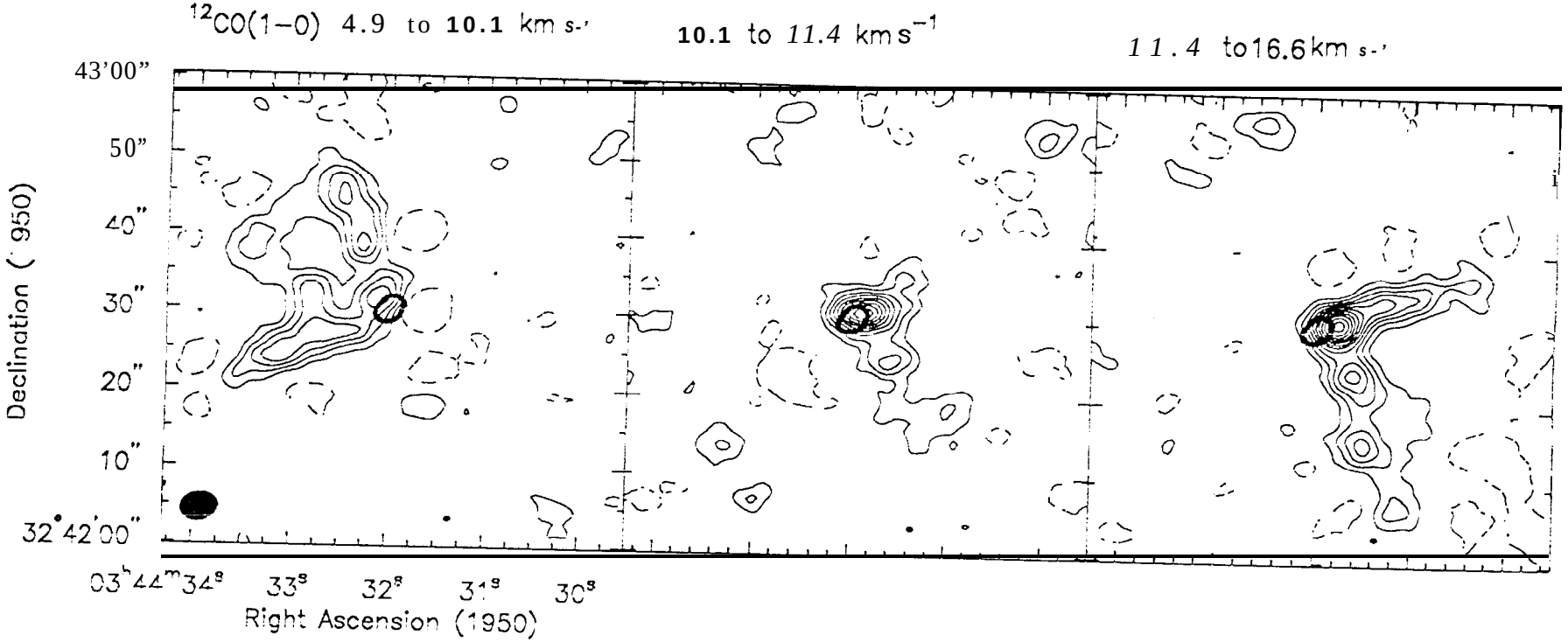
^{12}CO(1–0) 4.9 to 10.1 km s^{-1}
10.1 to 11.4 km s^{-1}
11.4 to 16.6 km s^{-1}
43'00"
50"
40"
30"
20"
10"
32°42'00"
Declination (1950)
03h44m34s
33s
32s
31s
30s
Right Ascension (1950)

Fig. 2

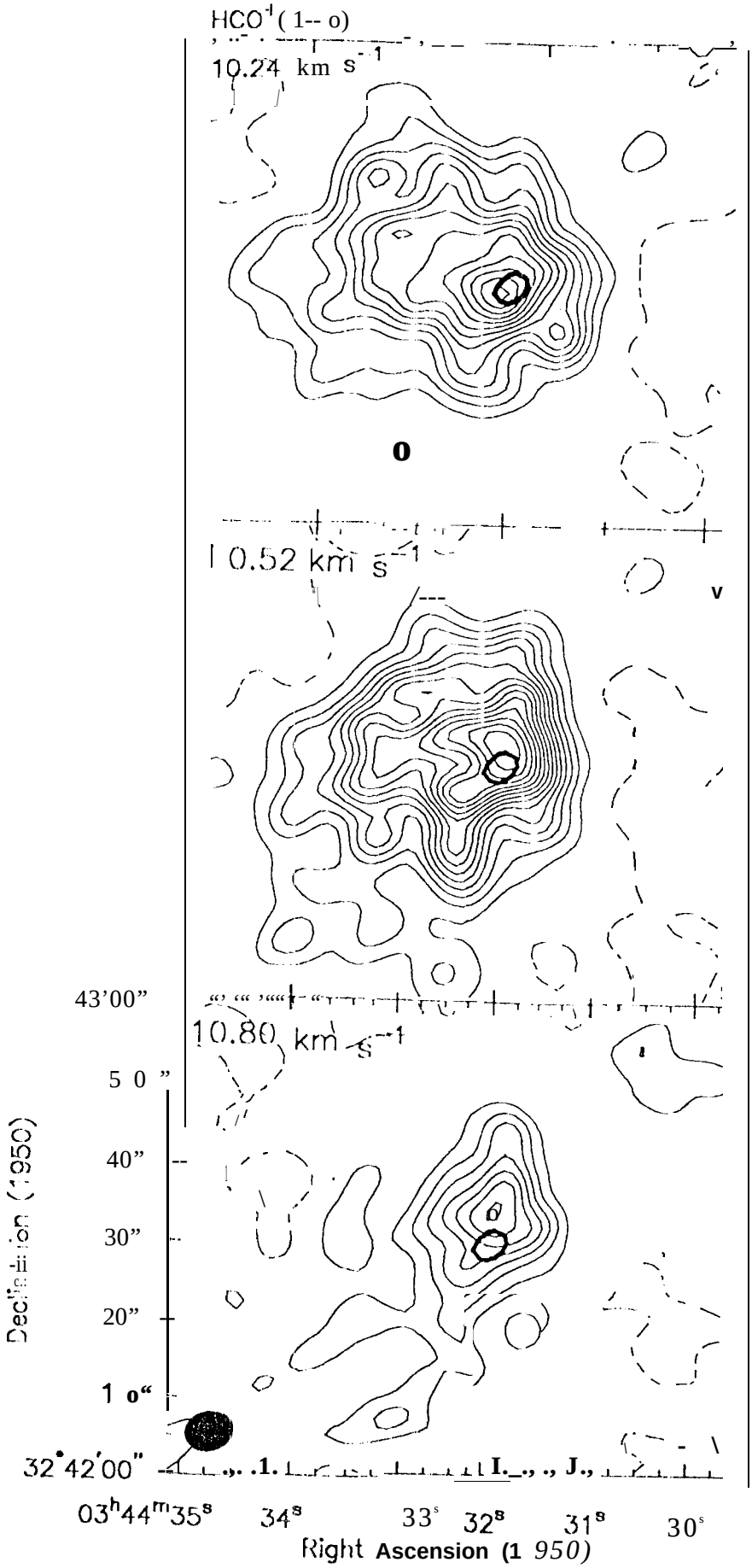
HCO+ (1-- o)
10.24 km s-1
0
10.52 km s-1
v
43'00"
10.80 km s-1
5 0 "
40"
30"
20"
1 o"
32°42'00"
03h44m35s
34s
33s
32s
31s
30s
Right Ascension (1950)

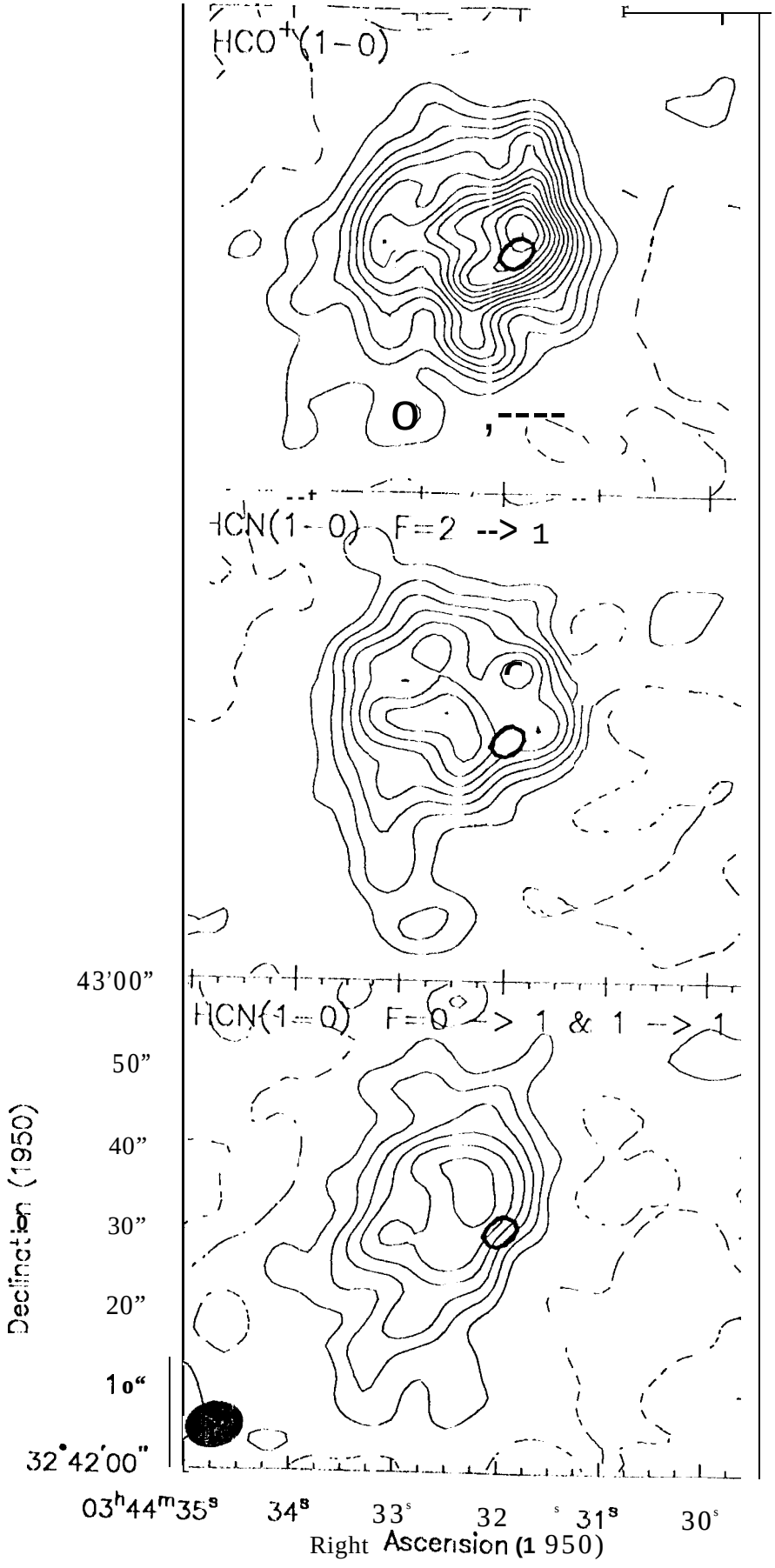
HCO+(1-0)
HCN(1-0) F=2 --> 1
HCN(1-0) F=0 --> 1 & 1 --> 1
43'00"
50"
40"
30"
20"
10"
32°42'00"
Declination (1950)
03h44m35s
34s
33s
32s
31s
30s
Right Ascension (1950)

Fig. 4

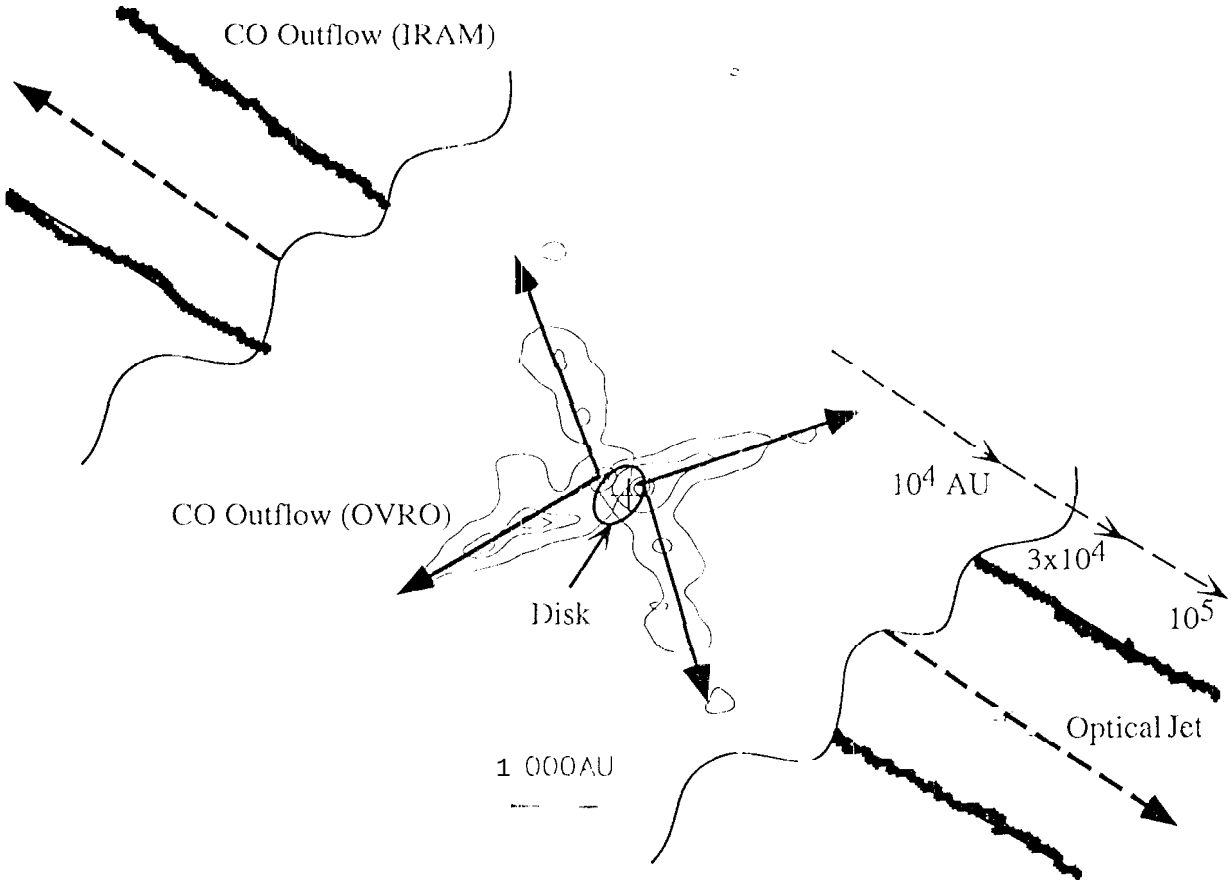
CO Outflow (IRAM)
CO Outflow (OVRO)
Disk
1 000AU
10^4 AU
$3x10^4$
10^5
Optical Jet

Figure 5